Regional Characteristics of Cloud Radiative Effects before and after the South China Sea Summer Monsoon Onset

Man HUANG[1], Jiandong LI[2*], Gang ZENG[1], and Yongkun XIE[3]

1 *Key Laboratory of Meteorological Disaster of Ministry of Education (KLME), Collaborative Innovation Center on Forecast and Evaluation of Meteorological Disasters (CIC-FEMD), Nanjing University of Information Science & Technology, Nanjing* 210044

2 *State Key Laboratory of Numerical Modeling for Atmospheric Sciences and Geophysical Fluid Dynamics, Institute of Atmospheric Physics, Chinese Academy of Sciences, Beijing* 100029

3 *Collaborative Innovation Center for Western Ecological Safety, Lanzhou University, Lanzhou* 730000

(Received April 27, 2020; in final form October 9, 2020)

ABSTRACT

The South China Sea summer monsoon (SCSSM) onset is characterized by rapid thermodynamical changes in the atmosphere that are critical to regional weather and climate processes. So far, few studies have focused on the changes in the associated cloud and radiative features. This study investigates spatiotemporal characteristics of top-of-atmosphere (TOA) cloud radiative effects (CREs) before and after the SCSSM onset over the South China Sea (SCS) and South China (SC), based on the 2001–2016 Clouds and the Earth's Radiant Energy System (CERES) Energy Balanced and Filled (EBAF) satellite data and ERA-Interim reanalysis data. Before the SCSSM onset, strong net CRE (NCRE) dominated by its cooling shortwave component occurs over SC, while descending motion and weak NCRE prevail over the SCS. In the SCSSM onset pentad, convection, high clouds, and longwave and shortwave CREs (LWCRE and SWCRE) abruptly increase over the southern and central SCS, and their high-value centers subsequently move northeastward and are strongly affected by the western Pacific subtropical high. The strong offset between LWCRE and SWCRE enables the NCRE intensity (TOA radiation budget) to be quite small (large) between the SCS and the western North Pacific after the SCSSM onset. In contrast, low–middle-level clouds and strong cooling SWCRE remain over SC after the SCSSM onset, but the increasing high clouds and LWCRE weaken (intensify) the regional NCRE (TOA radiation budget) intensity. These marked latitudinal differences in CREs between the SCS and SC primarily arise from their respective dominant cloud types and circulation conditions, which manifest the differences between the tropical SCSSM and subtropical East Asian monsoon processes. The results indicate that regional cloud fractions and CREs before and after the SCSSM onset are strongly modulated by quickly changed large-scale circulation over the East Asian monsoon regions, and the spatiotemporal variation of CREs is a response to the monsoonal circulation adjustment to a large extent.

Key words: cloud radiative effects (CREs), top-of-atmosphere (TOA) radiation budget, South China Sea summer monsoon (SCSSM), South China (SC)

Citation: Huang, M., J. D. Li, G. Zeng, et al., 2020: Regional characteristics of cloud radiative effects before and after the South China Sea summer monsoon onset. *J. Meteor. Res.*, **34**(6), 1167–1182, doi: 10.1007/s13351-020-0018-6.

1. Introduction

The South China Sea summer monsoon (SCSSM) is an important component of the Asian monsoon, prevailing over the South China Sea (SCS) and the Philippines (Tao and Chen, 1987; Lau and Yang, 1997; Wu and Wang, 2001; Ding and Chan, 2005). The SCSSM usually erupts in May and its onset is accompanied by abrupt changes in atmosphere circulation and regional precipitation amount, signifying the beginning of the summer monsoon over East Asia and the adjacent western Pacific Ocean (Lau and Yang, 1997; Liu et al., 1998; Wang et al., 2004). The SCS is one of the key water vapor source areas for South China (SC). Anomalous con-

Supported by the National Key Research and Development Program of China (2017YFA0603503 and 2017YFA0603804), National Natural Science Foundation of China (41831174, 41975109, and 41730963), and UK–China Research and Innovation Partnership Fund through the Met Office Climate Science for Service Partnership (CSSP) China as part of the Newton Fund.

*Corresponding author: lijd@mail.iap.ac.cn.

© The Chinese Meteorological Society and Springer-Verlag Berlin Heidelberg 2020

(C)1994-2021 China Academic Journal Electronic Publishing House. All rights reserved. http://www.cnki.net

vection over the SCS and the Philippines may have major impacts on the springtime and summertime occurrence of drought and flood over SC (Huang, 1990; Li et al., 2016). Investigation of the SCSSM activities has been an important task for monitoring and predicting the summer precipitation over East Asia, especially over SC, which is immediately adjacent to the SCS (Ding et al., 2006; Zhu et al., 2007). In-depth understanding of the climatic processes associated with the SCSSM onset is essential to regional weather forecast and climate prediction over the East Asian monsoon regions.

Numerous studies have shown that large-scale circulation conditions display rapid changes before and after the SCSSM onset. For instance, the western Pacific subtropical high suddenly weakens and retreats eastward to east of the Philippines, while the South Asian anticyclone moves westward to the Indochina Peninsula after the SCSSM onset. The low-level easterly wind is dramatically replaced by the westerly wind and strong convective activities quickly increase over the SCS (Wang et al., 2004; He et al., 2007). Local-scale cloud–precipitation characteristics, such as cloud fraction and vertical structure, cloud top bright temperature, and raindrop size distribution, also show pronounced variation with the SCSSM onset (Tanaka, 1992; Qian and Yang, 2000; Wu, 2002; Hu et al., 2011; Ren and Fang, 2013; Zeng et al., 2019). Notably, cloud physical properties and resultant cloud radiative effects (CREs) representing bulk cloud radiative roles in the surface-atmosphere system (Ramanathan et al., 1987; Allan, 2011) are very sensitive to circulation conditions (Rogers and Yau, 1989; Bony et al., 2015), and they are easily influenced by rapid variations of circulation accompanying the SCSSM onset. Meanwhile, clouds play key roles in modulating the atmospheric radiation budget and heating, and the uneven distribution of regional radiation energy is one of the main drivers for the atmosphere circulation (Webster et al., 1998; Trenberth et al., 2009). It is therefore critical to investigate regional spatiotemporal characteristics of CREs associated with the SCSSM onset.

It is noteworthy that although seasonal variation of cloud fraction and its vertical distribution over the Asian monsoon regions are strongly influenced by the monsoon march (Luo et al., 2009; Guo and Zhou, 2015; Zhang et al., 2020), considerable differences in cloud types and CREs appear over tropical and subtropical Asian monsoon regions (Yu et al., 2001; Luo et al., 2009; Li et al., 2017). Li et al. (2019) showed that strong and persistent cloud radiative cooling stays over SC from late winter to early summer, while a notably weak counterpart occurs over the SCS, but the intensity of CREs over these two subregions is enhanced with the SCSSM onset. In fact, subseasonal evolution of regional atmospheric circulation and resultant precipitation also markedly differs between the tropical SCS and subtropical SC (He et al., 2007, 2008; Zhao et al., 2007, 2008; Zhu et al., 2011). Further identifying differences in CREs over the SCS and its adjacent SC during the SCSSM onset is therefore an interesting issue for clearly revealing the subseasonal evolution of tropical SCSSM and subtropical East Asian monsoon. However, compared with large-scale atmospheric circulation changes, which have been extensively investigated by a great variety of studies, research on characteristics of CREs related to the SCSSM onset remains deficient over the SCS, SC, and their surrounding regions. Little is known to date about key characteristics of regional CREs over the SCS and adjacent SC regions, their influences on top-of-atmosphere (TOA) radiation budget, and their differences before and after the SCSSM onset. This kind of knowledge gap hinders an in-depth understanding of cloud roles in the regional surface-atmosphere energy budget and relevant climatic processes. The present study aims to address the aforementioned issues and to provide necessary observational information to further explore the potential influences of clouds on the SCSSM process.

This paper is organized as follows. Section 2 introduces the data and methods. Section 3 presents the climatological pentad mean states of circulations, cloud fractions, CREs, and TOA radiation budget in May, and analyzes their possible associations over the SCS and adjacent regions. Section 4 shows the pentad evolution of the above mentioned variables before and after the SCSSM onset and compares their differences between the SCS and SC regions. Section 5 selects two case years to investigate further the characteristics of regional CREs before and after the SCSSM onset and their differences in these two years. Finally, Section 6 presents the conclusions and discussion.

2. Data and methods

2.1 *Data*

The daily radiative flux and cloud fraction data used in this study are NASA's Clouds and the Earth's Radiant Energy System (CERES) Energy Balanced and Filled (EBAF) Ed2.8 dataset from March 2000 to December 2016 (Loeb et al., 2009; Doelling et al., 2013). The CERES-EBAF includes TOA incident shortwave radiative flux, outgoing shortwave and longwave radiative fluxes under clear-sky and all-sky conditions, as well as total, high, and low cloud fractions. More information

(C)1994-2021 China Academic Journal Electronic Publishing House. All rights reserved. http://www.cnki.net

about CERES-EBAF data (e.g., retrieval algorithm, processing methods, and data quality) can be accessed at http://ceres.larc.nasa.gov. The precipitation data are from the Global Precipitation Climatology Project (GPCP; Adler et al., 2003). The meteorological data are from the ECMWF interim reanalysis (ERA-Interim) dataset (Dee et al., 2011). The CERES-EBAF data have a spatial resolution of 1.0° (latitude) × 1.0° (longitude), and the 1.0°× 1.0° resolution versions of other datasets are also chosen. The datasets mentioned above are considered the observations in this study.

2.2 *Methods*

This study adopted the definition of the SCSSM onset by Wang et al. (2004) to determine the onset pentad of the SCSSM for the climatological mean and individual years. The key variable in Wang's definition is the 850-hPa zonal wind averaged over the central SCS (5°–15°N, 110°–120°E). Please refer to the work by Wang et al. (2004) for additional details. This criterion of the SCSSM onset depicts well not only the sudden establishment of the SCSSM but also the outbreak of the rainy season in the central–northern SCS and is thus widely used in climatic studies associated with the SCSSM onset. Following Wang's definition, pentad 27 is calculated to be the climatological mean SCSSM onset pentad during 2001–2016.

The CRE, which is defined as the difference in TOA radiative fluxes between clear-sky and all-sky conditions, can well represent the bulk radiative effects of clouds on the surface-atmosphere system (Ramanathan, 1987; Allan, 2011). CREs are divided into warming longwave CRE (LWCRE) and cooling shortwave CRE (SWCRE). The net CRE (NCRE) is the arithmetic sum of LWCRE and SWCRE to represent the total CRE at the TOA. CREs are widely used in current research on cloud–radiation processes, model evaluation, and climate uncertainties (Boucher et al., 2013). The formulas of CREs are as follows:

$$\mathrm{LWCRE} = \mathrm{OLRCS} - \mathrm{OLR}, \tag{1}$$

$$\mathrm{SWCRE} = \mathrm{RSUTCS} - \mathrm{RSUT}, \tag{2}$$

$$\mathrm{NCRE} = \mathrm{LWCRE} + \mathrm{SWCRE}, \tag{3}$$

where OLRCS and OLR are outgoing longwave radiation fluxes at the TOA under clear-sky and all-sky conditions, respectively; RSUTCS and RSUT are the corresponding outgoing shortwave radiation fluxes. Note that the sign of SWCRE is negative and its increase denotes that the SWCRE intensity weakens. The same applies to NCRE except for high surface albedo regions.

To analyze the relative importance of cloud radiative cooling effect, we use a parameter named the ratio of CREs (CR), and its formula is listed below (Cess et al., 2001):

$$\mathrm{CR} = |\mathrm{SWCRE}/\mathrm{LWCRE}|. \tag{4}$$

If CR is close to 1.0, SWCRE and LWCRE can almost cancel out. If CR is obviously larger than 1.0, the SWCRE cooling effect is dominant relative to the LWCRE warming effect. Moreover, the TOA radiation budget (Rt) represents the net TOA energy of surface-atmosphere system and is strongly influenced by CREs. The Rt is calculated by the following equation (Trenberth et al., 2009):

$$\mathrm{Rt} = \mathrm{RSDT} - \mathrm{RSUT} - \mathrm{OLR}, \tag{5}$$

where RSDT represents TOA incident shortwave radiative flux. In addition, the apparent heat source (Q1) is computed by the method of Yanai et al. (1973) to describe the whole atmospheric heat source. Generally, ascending motion produces condensational heating with positive Q1, and descending motion causes evaporative cooling with negative Q1. OLR is also used to represent the strength of strong convective development over the tropical regions (Liu et al., 1998; Wu, 2002). The intensity of NCRE and Rt denotes their absolute values in this study. The abbreviations of variable names used in this study are listed in Table 1.

The period of January 2001 to December 2016 is selected to match the common periods of the abovementioned data. The climatological pentad (5 days) average is adopted to analyze the subseasonal variation, which is effective for avoiding the synoptic-scale disturbance (Lau and Yang, 1997; He et al., 2007). The daily cloud fractions, CREs, Rt, and other relevant meteorological variables are averaged into pentad mean records. In this study, SC covers the Chinese mainland regions south of 32°N.

3. Geographical distribution of pentad mean states in May

The SCSSM exhibits quite pronounced subseasonal variability in circulation and precipitation. In this section, we present the geographical distribution of pentad mean circulation and cloud–radiation variables to examine their features associated with the abrupt SCSSM onset. Pentads 25–30 range from April 30 to May 29, covering most pentads in May, which is generally the SCSSM onset month, and approximately represent the May period in this study.

(C)1994-2021 China Academic Journal Electronic Publishing House. All rights reserved. http://www.cnki.net

Table 1. Abbreviations of variable names used in this study

Variable name	Physical meaning	Unit	Sign
TOA	Top of atmosphere	/	/
LWCRE	Longwave cloud radiative effect	W m^{-2}	+
SWCRE	Shortwave cloud radiative effect	W m^{-2}	−
NCRE	Net cloud radiative effect	W m^{-2}	Generally negative
CR	Absolute value of the ratio of SWCRE to LWCRE	/	+
OLR	Outgoing longwave radiative flux at the TOA under all-sky conditions	W m^{-2}	+
OLRCS	Outgoing longwave radiative flux at the TOA under clear-sky conditions	W m^{-2}	+
RSDT	Incident solar radiation at the TOA	W m^{-2}	+
RSUT	Outgoing shortwave radiative fluxe at the TOA under all-sky conditions	W m^{-2}	+
RSUTCS	Outgoing shortwave radiative fluxe at the TOA under clear-sky conditions	W m^{-2}	+
Q1	Apparent heat source	W m^{-2}	Region dependent
Rt	Radiation budget (equal to net radiative flux) at the TOA	W m^{-2}	Region dependent
W_{500}	500-hPa vertical velocity	hPa day^{-1}	−
HCF	High cloud fraction	%	+
TCF	Total cloud fraction	%	+
SC	South China	/	/
SCS	South China Sea	/	/
SCSSM	South China Sea summer monsoon	/	/

In pentads 25–26, the western side of the subtropical high reaches into the SCS, where low-level easterly wind prevails; weak descending motion occurs over the central SCS (Figs. 1a, b) and is accompanied by high OLR with a value up to 270 W m^{-2}, quite weak precipitation, and Q1 (see Figs. S1a, b, g, h in the online supplemental material), indicating that local strong convective activities are suppressed. In contrast, considerable ascending motion (up to −40 hPa day^{-1}) occurs over SC, which is only located south of the high-level westerly jet; and the low-level westerly wind from the Bay of Bengal and southerly wind from the SCS come into SC (Figs. 1a, b). At this time (pentads 25–26), large amounts of high cloud fraction (HCF) occur in the southern Indochina, Maritime Continent, and western tropical Pacific, but HCF is very small over the SCS and SC (Figs. 2a, b). Total cloud fraction (TCF) is very large over SC and is mainly contributed by low–middle-level clouds (Figs. 2a, b, g, h). The intensities of LWCRE and SWCRE are quite weak over most of the SCS, leading to a weak NCRE with only a value of −10 to 0 W m^{-2} (Figs. 3a, b, g, h; 4a, b). Obviously positive TOA Rt (up to 100 W m^{-2}) occurs between the SCS and the western North Pacific. Conversely, very large SWCRE (up to −120 W m^{-2}) and NCRE (Figs. 3a, b) occur over SC, corresponding to high CR (> 3.0; Figs. S2a, b), and the spatial centers of high SWCRE, CR, and NCRE are close (Figs. 3a, b; 4a, b; and Fig. S1a, b). This pattern demonstrates that the SWCRE has a dominant role in regional CREs. The large SWCRE intensity over SC is closely related to the above mentioned circulation conditions before the SCSSM onset and the thermodynamic effects induced by the Tibetan Plateau orography (Wu et al., 2007; Yu et al., 2001; Li et al., 2019). Particularly, the high-level westerly jet acts as a pumping unit for stimulating regional ascending motion, and the low-level westerly and southerly wind not only produce cyclonic convergence but also bring abundant water vapor into SC. These circulation conditions favor the generation and maintenance of low–middle-level clouds, which can strongly reflect shortwave radiation and cause large SWCRE (Li et al., 2019). Due to the strong shortwave radiative cooling of clouds, pronounced weak TOA Rt with intensity nearly equal to 0 W m^{-2} appears over SC and coincides well with the spatial pattern of NCRE (Figs. 4a, b).

In the SCSSM onset pentad (pentad 27), the low-level easterly wind is abruptly shifted into westerly wind accompanied by eastward displacement of the subtropical high (Fig. 1c). Meanwhile, strong ascending motion, HCF, and TCF suddenly appear over the central SCS (Figs. 1c; 2c, i). Correspondingly, LWCRE and SWCRE also suddenly intensify over the SCS, but they strongly offset each other, causing NCRE to be only slightly enhanced. Unlike SCS, the evident ascending motion and cloud fractions change little over SC, so are the large-value areas of LWCRE, SWCRE, and NCRE.

In pentads 28–30, intensified southwesterly wind is across the Indochina Peninsula, reaching the SCS and SC regions; and the ascending motion extends to the whole SCS, with its center advancing northeastward between central SCS and North Philippines (Figs. 1d–f). Meanwhile, the subtropical high further withdraws eastward and its central position moves northward. The 200-hPa westerly jet weakens and moves northwestward. In pentads 29–30, the increased convection and high and total cloud amounts are coincident with intensified LW-

(C)1994-2021 China Academic Journal Electronic Publishing House. All rights reserved. http://www.cnki.net

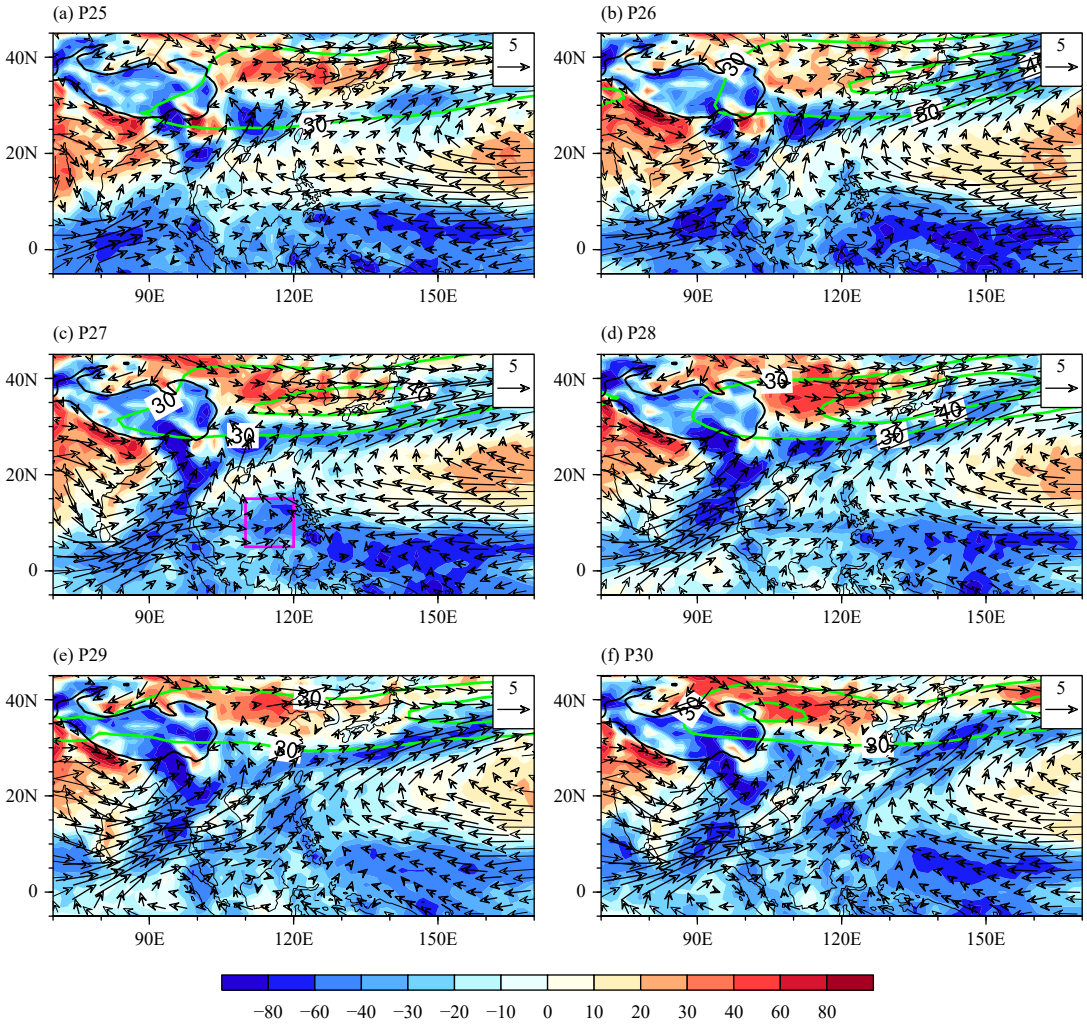

Fig. 1. Geographical distributions of circulation in pentads 25–30 during 2001–2016. In (a), the shading is 500-hPa vertical velocity (hPa day^{-1}), the green line is 200-hPa westerly jet, and the vector is 850-hPa wind (m s^{-1}) masked below 850 hPa. The solid black line is the Tibetan Plateau (over 3000 m). The red box in Fig. 1c represents the domain that is used to define the South China summer monsoon (SCSSM) onset.

CRE and SWCRE between the central SCS and North Philippines (Figs. 1e, f; 2e, f; 3e, f). In the meantime, strong descending motion prevails over the subtropical high regions, corresponding to small TCF and very weak LWCRE and SWCRE; and clear ascending motion occurs to the southern and northwestern sides of the subtropical high regions with large cloud fractions and strong LWCRE and SWCRE. The spatial distribution of descending (ascending) motion nearly coincides with weak (strong) LWCRE and SWCRE in the western Pacific regions. During the same period, considerable ascending motion and large SWCRE and NCRE remain over SC, but their intensity centers somewhat move westward with the enhanced southwesterly wind from the Bay of Bengal (Figs. 3e, f; 4e, f).

Figure 5 shows the differences in CREs and Rt between pentads 25–26 and 29–30. Remarkable increases in the intensities of LWCRE and SWCRE appear especially over the central and northern SCS after the SCSSM onset, and the westward movement of SWCRE intensity center is also very clear (Figs. 5a, b). Because of the strong offset between LWCRE and SWCRE, the NCRE intensity (cloud radiative cooling role) only increases by 10–20 W m^{-2} over the central to northern SCS, corresponding to slightly reduced Rt (Figs. 5c, d). Relatively, the intensities of LWCRE and SWCRE change less over SC because of its remaining circulation conditions. The changes in SWCRE over part of southeastern SC are mainly caused by the anticyclone and resultant descending motion.

Moreover, from June to mid-July, strong convection, LWCRE, and SWCRE display a northeastern advancement between the SCS and western North Pacific (figures omitted). This northeastward propagation is closely

(C)1994-2021 China Academic Journal Electronic Publishing House. All rights reserved. http://www.cnki.net

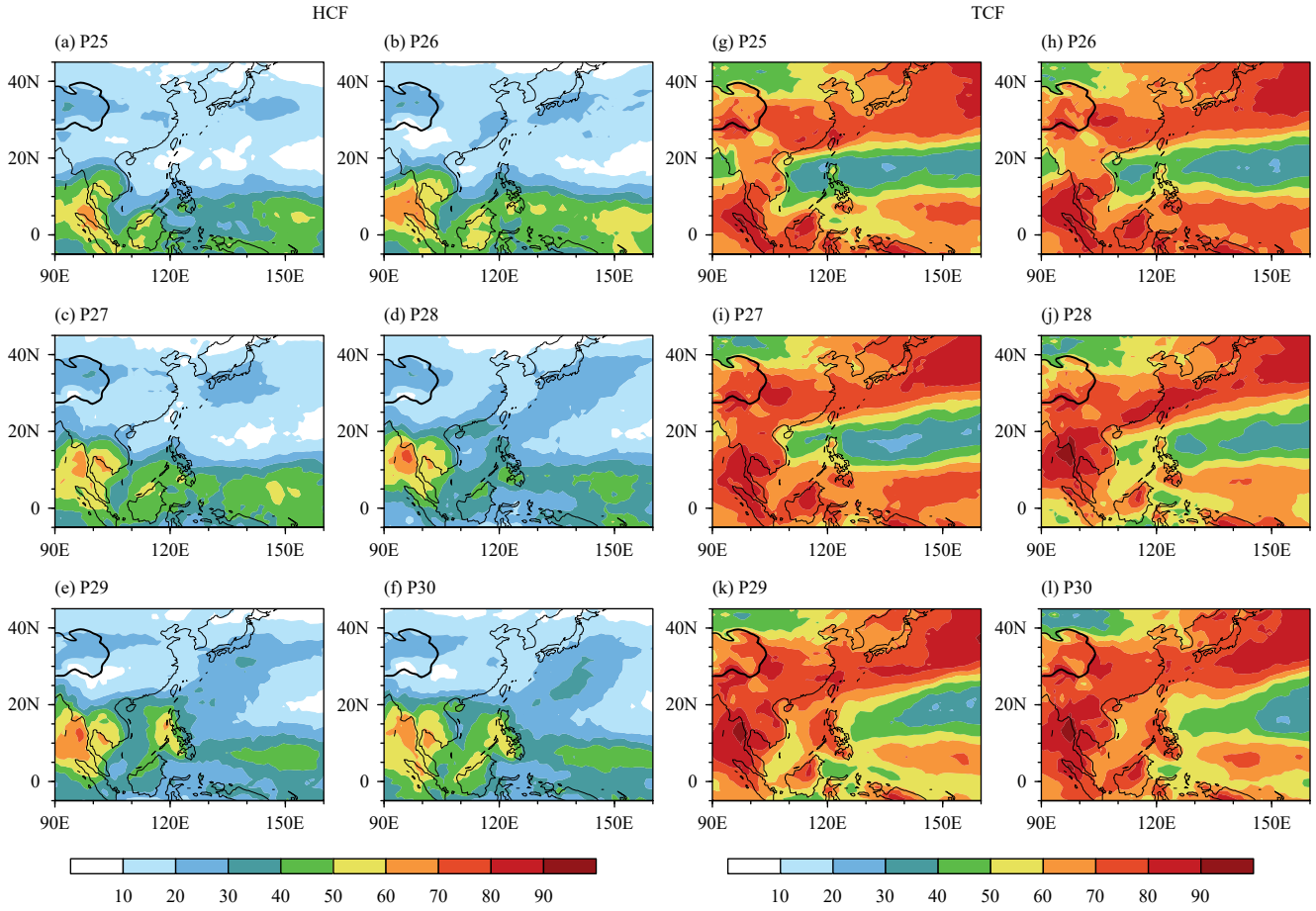

Fig. 2. Geographical distributions of (a–f) high cloud fraction (HCF; %) and (g–l) total cloud fraction (TCF; %) in pentads 25–30 during 2001–2016.

linked to the cloud–radiation and wind–evaporation feedbacks and the resultant sea surface temperature gradient induced by the SCSSM onset over the SCS, Philippine, and western North Pacific regions (Wu and Wang, 2001; Wu, 2002; Lau and Nath, 2009). These above mentioned spatiotemporal variations of vertical motion, cloud fractions, and CREs over the SCS, SC, and western North Pacific match well with the large-scale circulations before and after the SCSSM onset.

4. Temporal evolution of CREs with the SCSSM onset

The results shown in Section 3 indicate that the tropical SCS and subtropical SC possess quite different characteristics of circulation, dominant clouds, and CREs in May. In this section, subseasonal variations of zonal mean circulation, precipitation, and cloud–radiation variables averaged over 110°–120°E are examined to further compare their changes with the SCSSM onset at the SCS and SC latitudes.

As shown in Fig. 6, a sharp contrast before and after the SCSSM onset occurs at the SCS latitudes (approximately within 5°–20°N). After the SCSSM onset in pentad 27, the low-level westerly wind (larger than 1 m s^{-1}) rapidly outbreaks at the SCS latitudes, where the regional atmosphere dramatically changes from previous descending, dry, and cooling states into ascending, wet, and heating states (Figs. 6a–d). At this time, HCF, TCF, and the intensity of LWCRE and SWCRE also abruptly increase over the SCS (Figs. 6e, f; 7b, c).

Note that CR at most SCS latitudes somewhat decreases after the SCSSM onset and thereafter remains at a quite low value (< 1.4) because of gradually increased HCF and resultant LWCRE. The low CR value signifies the strong offset between LWCRE and SWCRE over the SCS, and the regional NCRE intensity is very weak accordingly (around −20 to −10 W m^{-2}). The low CR over the SCS is closely related to the tropical convection and cloud types. Over some tropical oceanic regions (e.g., tropical Pacific), strong and frequent convection activities lead to a relatively short cloud lifetime, and dominant

(C)1994-2021 China Academic Journal Electronic Publishing House. All rights reserved. http://www.cnki.net

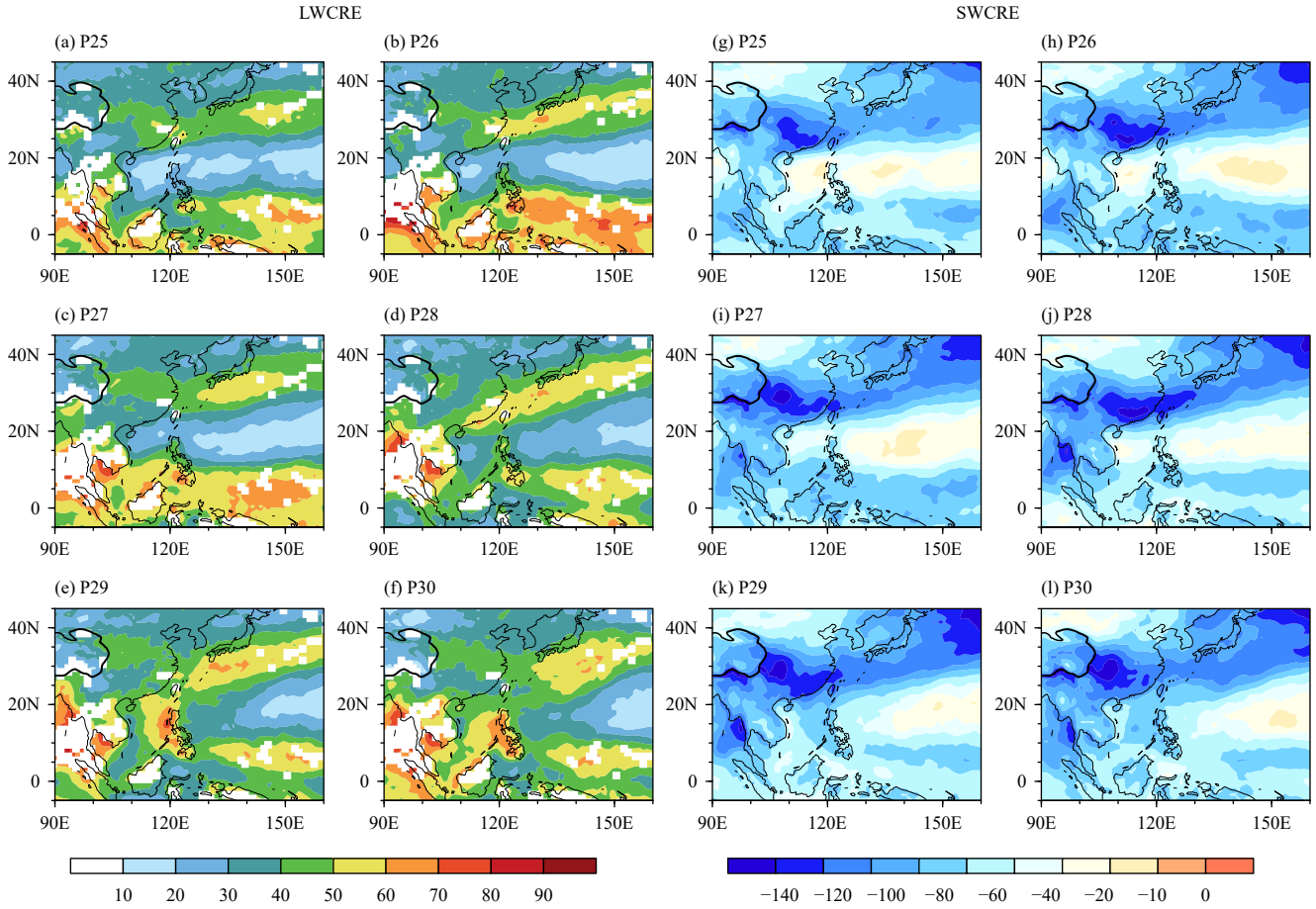

Fig. 3. Geographical distributions of (a–f) longwave cloud radiative effect (LWCRE; W m^{-2}) and (g–l) shortwave cloud radiative effect (SWCRE; W m^{-2}) in pentads 25–30 during 2001–2016.

high and total clouds favor the maintenance of strong and comparable LWCRE and SWCRE simultaneously, leading to the strong offset between LWCRE and SWCRE and a weak NCRE (Kiehl, 1994; Hartmann et al., 2001; Wall and Hartmann, 2018). The results shown in Figs. 4, 6 (and Fig. S2 in the online supplemental material) demonstrate that this offset feature is also pronounced over the SCS, except for tropical Pacific regions. Due to the weak cloud radiative cooling, positive Rt stays at high level with a peak value up to 110 W m^{-2} within 10°–20°N. It is noted that the intensified strong convection, precipitation, LWCRE, and SWCRE occur to the north of the increased westerly wind (Figs. 6b, c; 7b, c), which is caused by the spatial distribution of low-level convergence as interpreted by Wang et al. (2004) and Zhao et al. (2007).

In contrast to SCS latitudes, considerable ascending motion, wet, and heating atmospheric states maintain at SC latitudes (approximately 22°–30°N) from mid-March (pentad 15) to early May (pentad 24), which are accompanied by large CR (> 3.0) and strong SWCRE and NCRE. The persistent strong convection and precipitation over SC are generally considered to be caused by the subtropical East Asian summer monsoon, which markedly differs from the tropical SCSSM (He et al., 2007; Zhao et al., 2007, 2008). The ascending motion, precipitation, LWCRE, and SWCRE at SC latitudes are enhanced since pentad 24. These variations are closely related to the intensified southwesterly wind from the Bay of Bengal (Li et al., 2019) and the zonal thermal gradient reversal at the SCS latitudes since pentad 24 (He et al., 2007). With the SCSSM onset, the precipitation and LWCRE over SC display a southward movement (Figs. 6c, 7b), which is likely associated with the southward migration of the low-pressure trough east of the Tibetan Plateau (Zhao et al., 2008) and northeastward advance of the SCSSM convective center (Wu et al., 2002). However, SWCRE and NCRE do not obviously move southward like LWCRE but mainly stay between 22° and 30°N until late June when the favorable ascending motion and water vapor convergence quickly decrease as a result of the large-scale circulation changes over the Asian

(C)1994-2021 China Academic Journal Electronic Publishing House. All rights reserved. http://www.cnki.net

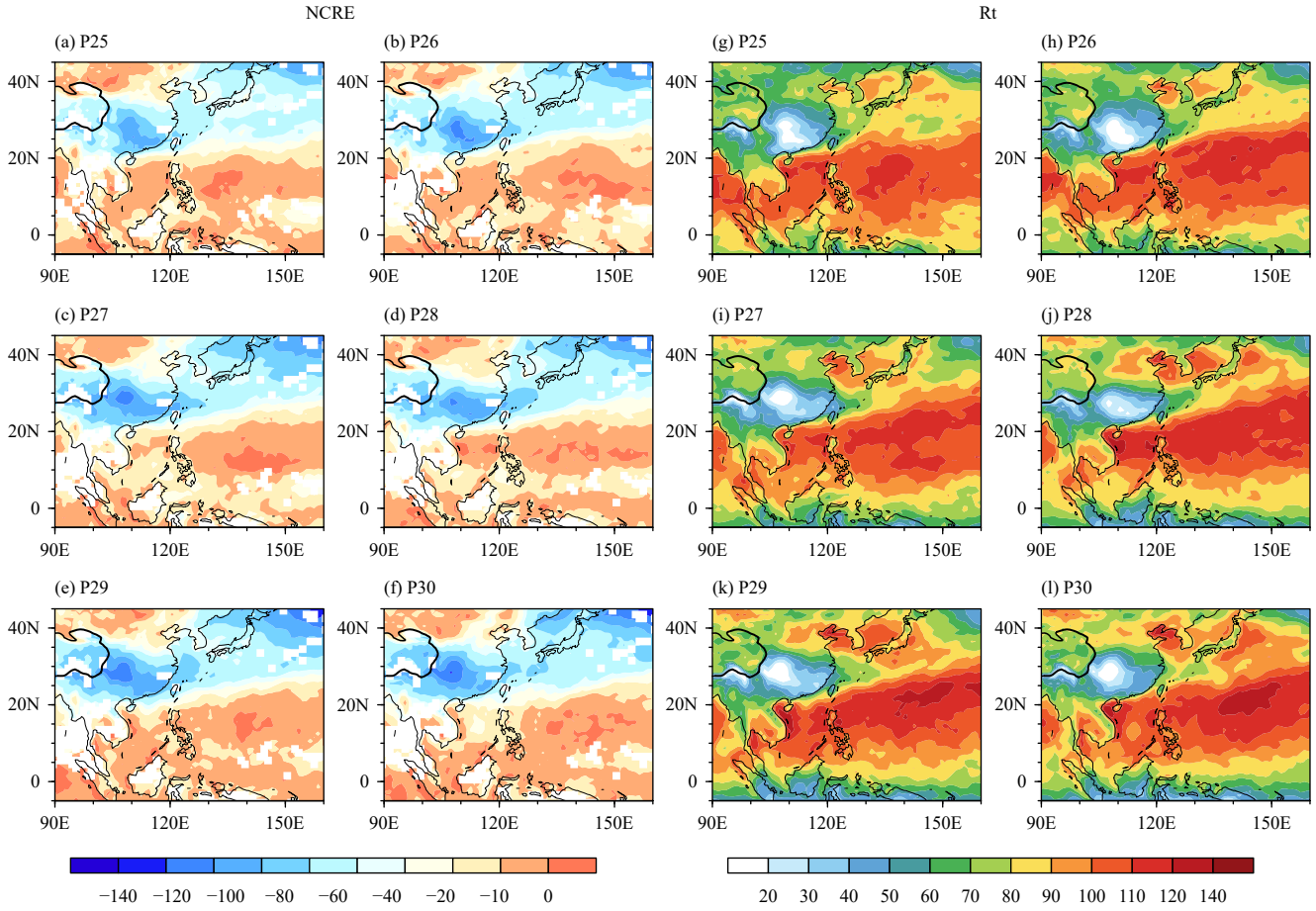

Fig. 4. Geographical distributions of (a–f) net cloud radiative effect (NCRE; W m^{-2}) and (g–l) top-of-atmosphere radiation budget (TOA Rt; W m^{-2}) in pentads 25–30 during 2001–2016.

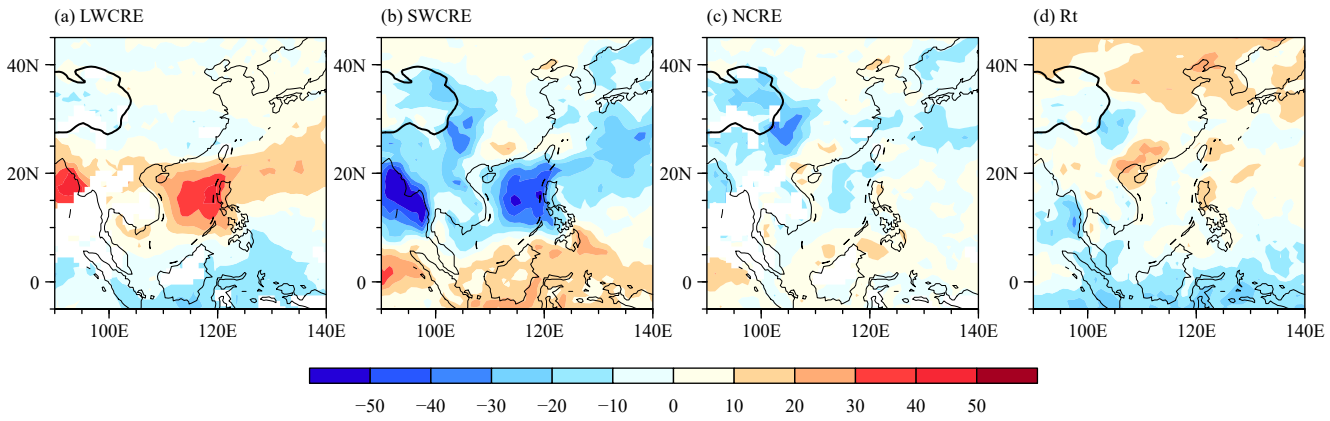

Fig. 5. Geographical distributions of the differences in (a) LWCRE (W m^{-2}), (b) SWCRE (W m^{-2}), (c) NCRE (W m^{-2}), and (d) Rt (W m^{-2}) between pentads 25–26 and 29–30 during 2001–2016.

monsoon regions (Li et al., 2019). Maintenance of strong NCRE (up to −60 W m^{-2}) causes weaker Rt over SC (less than 50 W m^{-2}) relative to its south and north sides until late June.

At SC latitudes, CR rapidly decreases from larger than 4.0 to approximately 3.0 since pentad 24 when LWCRE quickly increases, indicating the enhanced role of the cloud radiative warming. Notably, variations of CR and Rt at the SCS and SC latitudes are highly correlated (Table 2). This is also closely related to variations of cloud fractions and cloud types during the East Asian summer monsoon. From mid-March (pentad 18) to late

(C)1994-2021 China Academic Journal Electronic Publishing House. All rights reserved. http://www.cnki.net

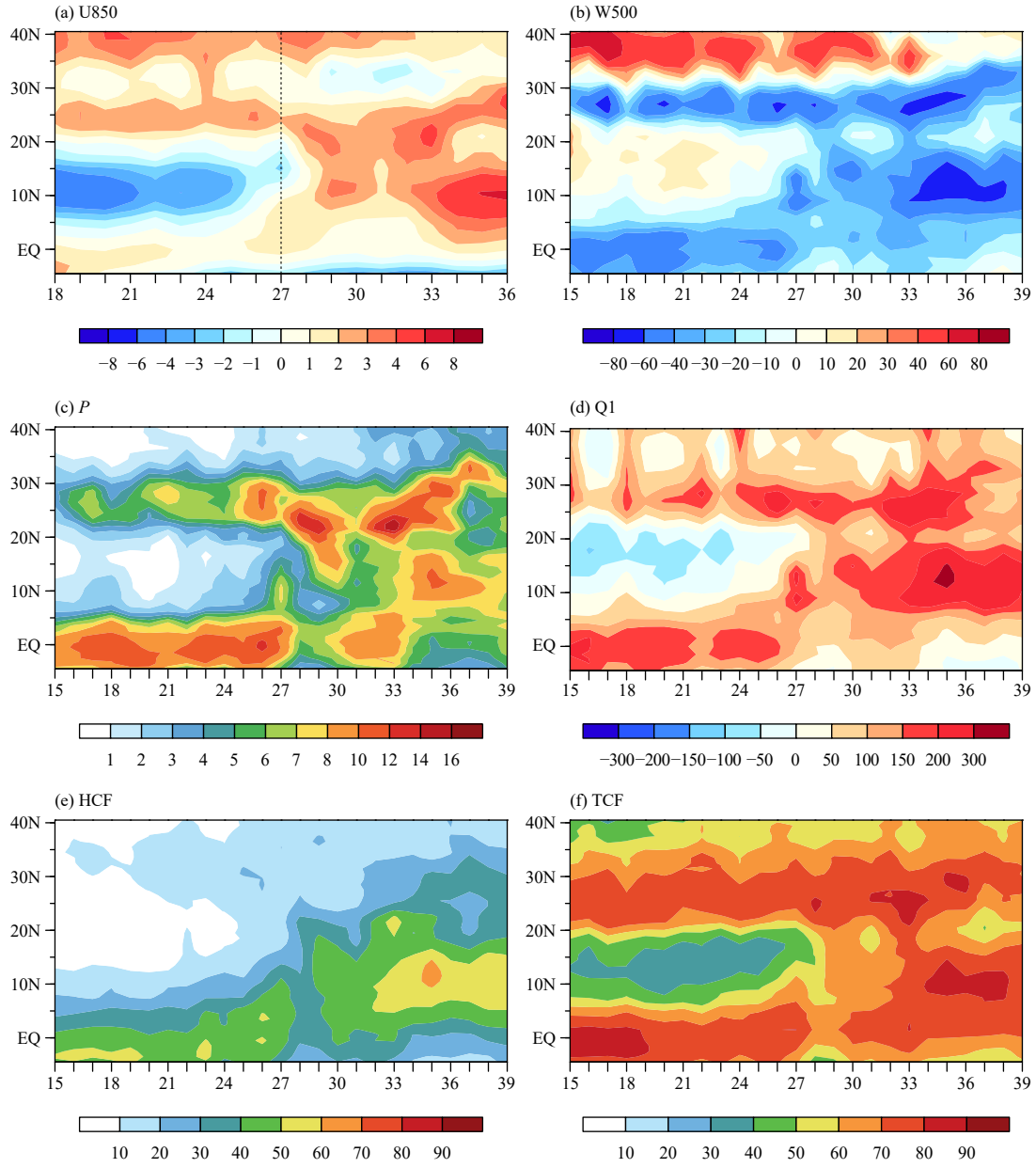

Fig. 6. Pentad mean changes in (a) 850-hPa zonal wind (U850; m s^{-1}), (b) 500-hPa vertical velocity (W500; hPa day^{-1}), (c) precipitation (P; mm day^{-1}), (d) OLR (W m^{-2}), (d) Q1 (W m^{-2}), (e) HCF (%), and (f) TCF (%) averaged over 110°–120°E in pentads 15–39 during 2001–2016. The x-axis denotes the pentad number. The black dashed line in (a) denotes the SCSSM onset pentad.

June (pentad 36), HCF and cloud top height gradually increase with the enhancement of convection and incident solar radiation (Fig. 7a) over SCS and SC, while large cloud fractions considerably contributed by low–middle-level clouds stay over SC. Thus, increased high clouds and the resultant cloud warming by LWCRE can reduce the net cloud radiative cooling effect. Thus, as mentioned in Section 2, the increase in CR can effectively represent the decrease (increase) in cloud radiative cooling (Rt) at the TOA, and the reverse is also true. As lis-

Table 2. Temporal correlation coefficients averaged over the SCS (10°–15°N, 110°–120°E) and SC (25°–30°N, 110°–120°E) regions in pentads 15–39 for 500-hPa vertical velocity (W_{500}) versus HCF (TCF), W_{500} versus LWCRE (SWCRE), CR versus Rt, and NCRE versus Rt, respectively

	SCS (10°–15°N)	SC (25°–30°N)
W_{500}–HCF	−0.980	−0.107
W_{500}–TCF	−0.976	−0.820
W_{500}–LWCRE	−0.990	−0.400
W_{500}–SWCRE	0.987	0.618
CR–Rt	−0.927	−0.976
NCRE–Rt	0.224	0.789

(C)1994-2021 China Academic Journal Electronic Publishing House. All rights reserved. http://www.cnki.net

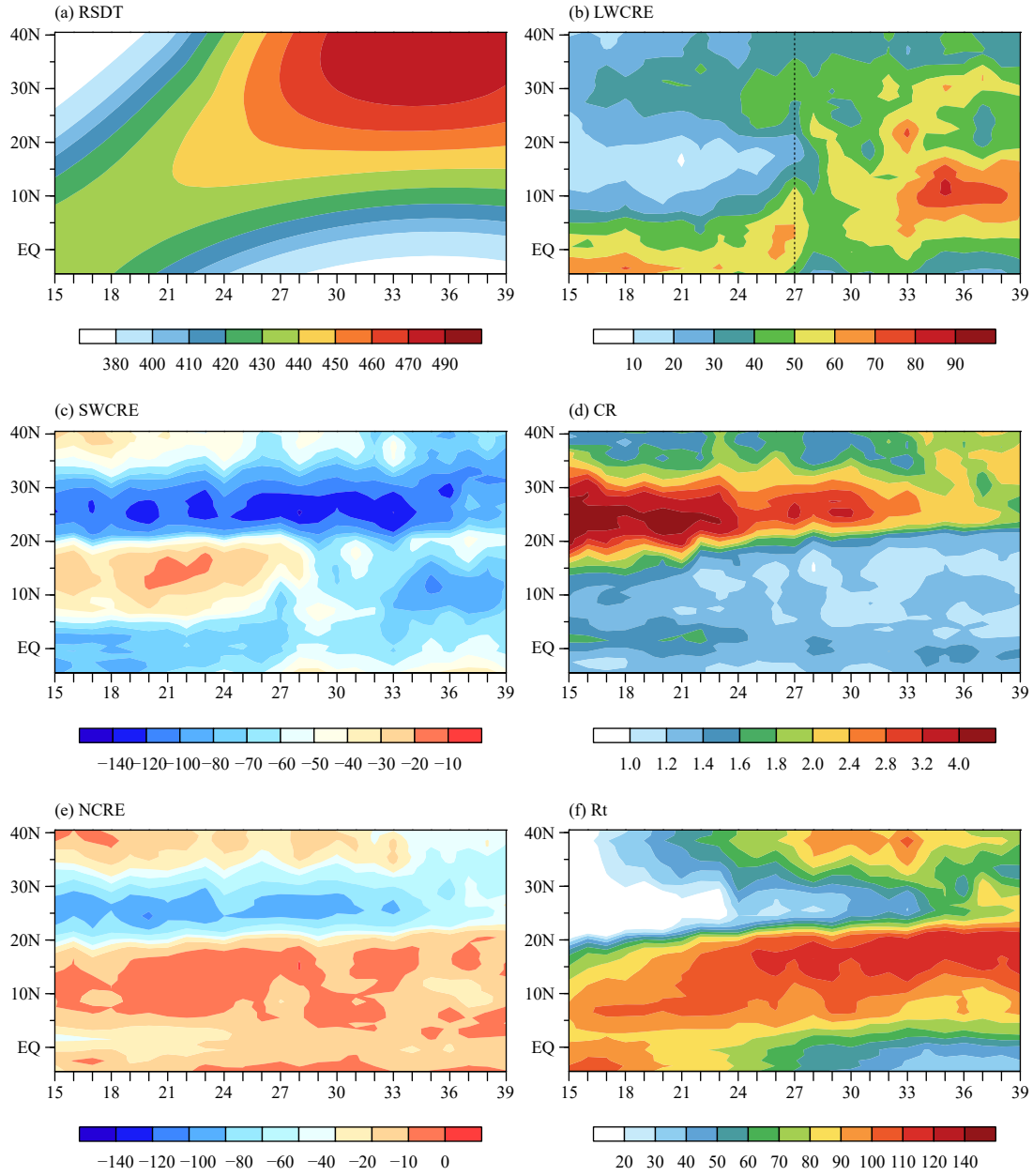

Fig. 7. Pentad mean changes in (a) RSDT (W m^{-2}), (b) LWCRE (W m^{-2}), (c) SWCRE (W m^{-2}), (d) CR, (e) NCRE (W m^{-2}), and (f) TOA Rt (W m^{-2}) averaged over 110°–120°E in pentads 15–39 of 2001–2016. The *x*-axis denotes the pentad number. The black dashed line in (b) denotes the SCSSM onset pentad.

ted in Table 2, the 500-hPa vertical velocity is highly correlated with HCF, TCF, LWCRE, and SWCRE over SCS, whereas its correlations with HCF and LWCRE are much lower over SC. The vertical motion (particularly at 500 hPa) is therefore an important connection between the local LWCRE and SWCRE intensity and the large-scale circulation over SCS. Relative to SCS, low–middle-level clouds also prevail over SC, where the cloud vertical structure is quite complex, although SWCRE is the dominant component of NCRE (Luo et al., 2009; Pan et al., 2015; Li et al., 2017). Unlike SCS, the low–middle-level ascending motion mainly contributes to low–middle-level clouds and the resultant strong SWCRE over SC, especially from spring to early summer (Li et al., 2020). In this situation, the 500-hPa vertical velocity only correlates well with TCF and SWCRE over SC, and the correlation between NCRE and Rt is also much better compared with that over SCS (Table 2).

The above mentioned different associations among vertical motion, cloud fraction, and CRE actually reflect the differences in clouds (dominant cloud type, cloud fraction, and their vertical distribution), CRE, and circu-

(C)1994-2021 China Academic Journal Electronic Publishing House. All rights reserved. http://www.cnki.net

lation conditions between the tropical SCSSM and subtropical East Asian summer monsoon.

5. The cases in 2011 and 2012

The SCSSM onset displays significant interannual variation (Wu and Wang, 2001; Wang et al., 2004). The pentad mean results during 2001–2016 may not reveal some of the evolution features of CREs before and after the SCSSM onset over our target regions. In this instance, 2011 and 2012 are respectively selected as late and early onset case years to compare further and to identify characteristics of regional CREs. The SCSSM onset pentads in 2011 and 2012 are pentads 29 and 25, respectively. It should be noted that evident 850-hPa westerly wind also appeared over the southern SCS in pentads 25–26 of 2011, but it did not extend to the central SCS until after pentads 27–28 (Figs. 8a, 9b). According to the onset criterion by Wang et al. (2004), the SCSSM actually broke out in pentad 29 of 2011.

Figures 8 and 9 present latitude–temporal variation of key circulation conditions, cloud fractions, CREs, and Rt in pentads 18–36 of 2011 and 2012, which cover the main period before and after the SCSSM onset in the two years. As clearly shown in Fig. 8, 850-hPa westerly wind and strong convection started to quickly and continuously increase over the central SCS since the onset pentad 29 (25) in 2011 (2012). In pentads 26–28 of 2011, when the SCSSM did not outbreak, convection, HCF, LWCRE, and SWCRE over the central and northern SCS (5°–20°N) are obviously weaker than their counterparts in 2012 (Figs. 8, 9). In pentads 29–30 of 2012, the SCSSM onset allows the intensity of convection, HCF, LWCRE, and SWCRE over the SCS to be obviously stronger than those in 2011. Over SCS, the differences in cloud fraction and CREs between the two years are mainly related to their regional ascending motion, which quickly enhanced with the SCSSM onset, giving rise to increased cloud fractions and resultant LWCRE and SWCRE. However, as mentioned in Section 3, CR is very low over SCS and results in strong offset between LWCRE and SWCRE. Accordingly, the difference in NCRE between 2011 and 2012 is considerably weaker than its longwave and shortwave components over SCS (Figs. 9c, g, k), and the Rt difference is similar to the NCRE difference (Figs. 9d, h, l).

Remarkable differences in the above variables also appear over SC especially before pentad 25, which is the SCSSM onset pentad in 2012. The 850-hPa westerly wind between 15° and 25°N and the 500-hPa ascending motion between 20° and 35°N are obviously weaker in May (pentads 19–24) of 2011 than their counterparts in 2012. Note that this difference in ascending motion between the two years is located north to that of 850-hPa westerly wind. The cause has been briefly explained in Section 3. Consequently, cloud fractions, LWCRE, and SWCRE in pentads 19–24 of 2011 are weaker than their counterparts in 2012 at SC latitudes (22°–32°N). Even after the offset of LWCRE and SWCRE, relative to 2011, NCRE and Rt over SC are still weaker in pentads 20–24 of 2012. At SC latitudes, another difference appears after pentad 29. In early and mid-June (pentads 31–34), increased ascending motion, which is due to the SCSSM onset, allows cloud fractions, LWCRE, and SWCRE in 2012 to be larger than those in 2011. Compared to the case over SCS, the differences in CREs over SC seem to be smaller, after the SCSSM late onset on pentad 29.

The above mentioned differences in circulation and CREs between 2011 and 2012 are closely associated with their individual large-scale circulation patterns. To compare further and to explain these circulation differences, Fig. 10 shows distributions of the large-scale circulations in three periods before and after the SCSSM onset in the two years. In pentads 19–23, compared with the situations in 2012, the 200-hPa westerly jet is stronger and its center is more north and west in 2011, and the western Pacific subtropical high is also more east and south. Thus, the ascending motion over SC is quite weak in 2011; conversely, the intensity of ascend motion and its spatial coverage over SC are obviously large in 2012. The stronger ascending motion over SC is favorable for more cloud fractions and larger CREs in pentads 19–23 of 2012. The cause of these differences is consistent with that found in recent studies (Li et al., 2019, 2020).

In pentads 26–28, the western Pacific subtropical high is more east and south in 2011 relative to 2012 (Figs. 10b, e, h). In this case, low-level westerly wind is inhibited into the SCS and local ascending motion is weaker in pentads 26–28 of 2012 while cloud fractions, LWCRE, and SWCRE are therefore larger. Analogously, a more west and northward location of the western Pacific subtropical high allows an evident anomalous anticyclone to occur between SC and southern Japan in pentads 31–35 of 2011 relative to 2012 (Figs. 10c, f, i). During this period, stronger ascending motion, increased cloud fraction, and larger LWCRE and SWCRE appear between northern SC and central China (Figs. 9i, j; 10c, f, i). Meanwhile, stronger ascending motion and weaker LWCRE and SWCRE appear over the central SCS and the Philippines, which are just located south to the anticyclone mentioned above.

The above case analyses further demonstrate that re-

(C)1994-2021 China Academic Journal Electronic Publishing House. All rights reserved. http://www.cnki.net

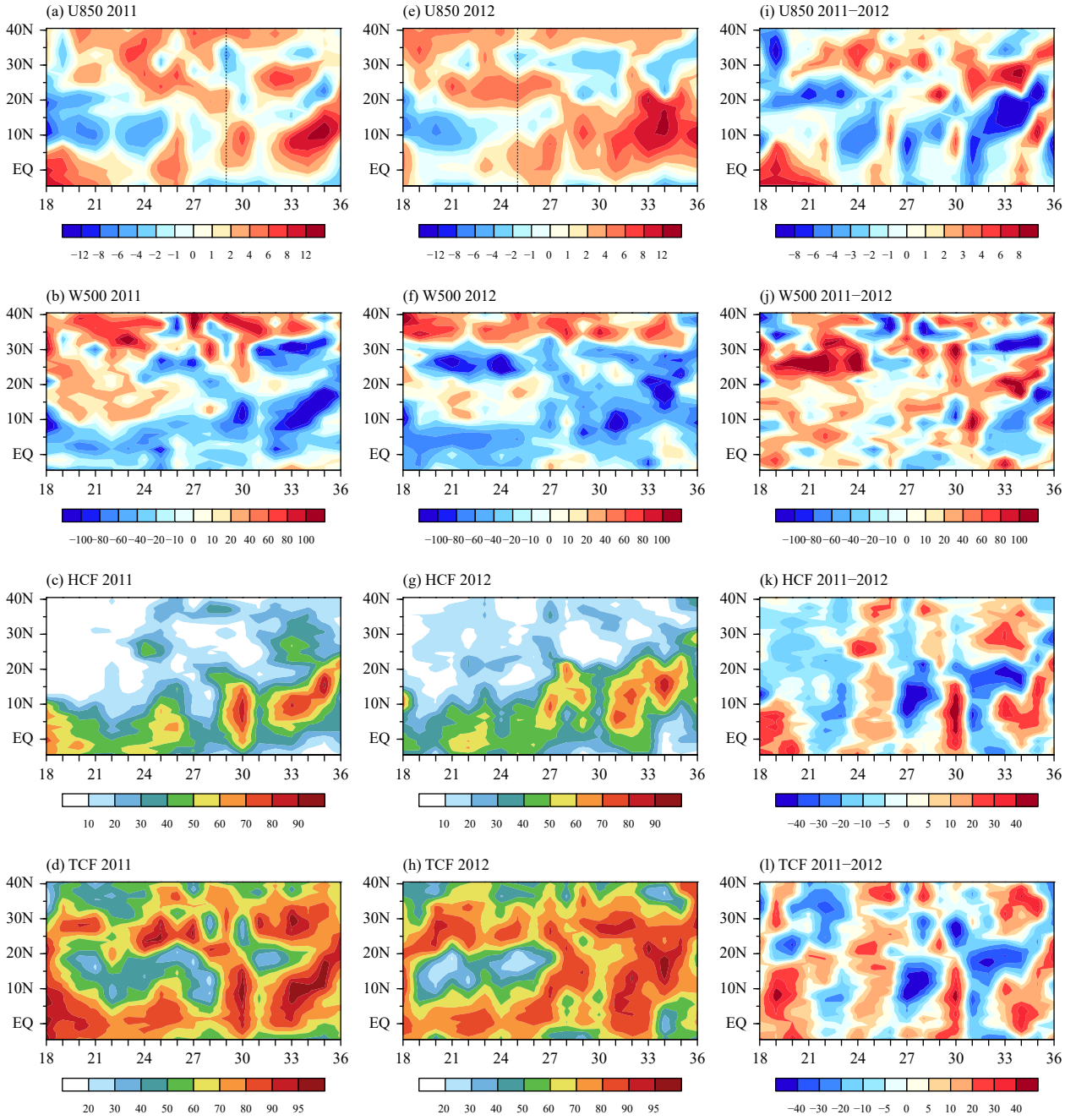

Fig. 8. Pentad mean changes in (a) 850-hPa zonal wind (U850; m s^{-1}), (b) 500-hPa vertical velocity (W500; hPa day^{-1}), (c) HCF (%), and (d) TCF (%) averaged over 110°–120°E in pentads 18–36 of 2011; (e–h) the counterparts in 2012; and (i–l) the differences between 2011 and 2012. The *x*-axis denotes the pentad number. The black dashed lines in (a, e) denote the SCSSM onset pentad in 2011 and 2012.

gional cloud fractions, LWCRE, and SWCRE over SCS abruptly increase just after the SCSSM onset. Over SC, the circulation distribution associated with the SCSSM onset allows the intensity and location of CREs in different case years to be obviously different before and after the SCSSM onset. Hence, before and after the SCSSM onset, variations in the intensity and location of regional CREs over the SCS and SC are the responses to the changes in large-scale atmospheric circulations over the Asian summer monsoon regions to a great extent. However, the SCSSM onset in individual years is affected by many factors, such as the intermittent southward intrusion of cold fronts into the northern SCS, the bogus onset in late April before the establishment of tropical monsoons over Indochina, and active intraseasonal oscillation (Wang et al., 2004). The results in this section are sensitive to the selected case years for the SCSSM onset. In this study, there are only 16-yr

(C)1994-2021 China Academic Journal Electronic Publishing House. All rights reserved. http://www.cnki.net

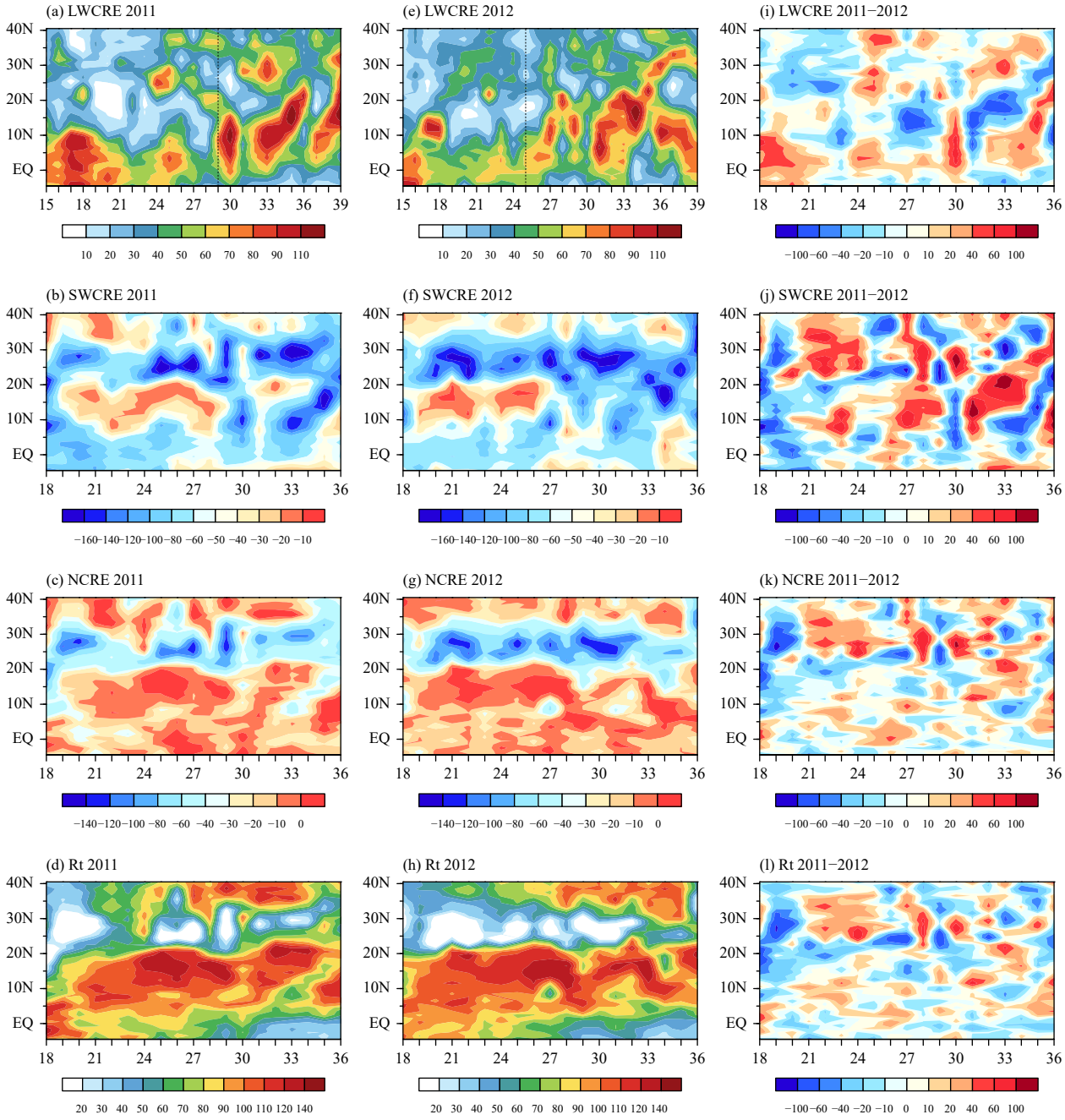

Fig. 9. Pentad mean changes in (a) LWCRE (W m^{-2}), (b) SWCRE (W m^{-2}), (c) NCRE (%), and (d) TOA Rt (W m^{-2}) averaged over 110°−120°E in pentads 18−36 of 2011; (e−h) the counterparts in 2012; and (i−l) the differences between 2011 and 2012. The *x*-axis denotes the pentad number. The black dashed lines in (a, e) denote the SCSSM onset pentad in 2011 and 2012, respectively.

CERES-EBAF satellite data matched with the ERA-Interim data period. More case analyses are still needed to investigate the interannual variation of regional CREs associated with the SCSSM onset.

6. Conclusions and discussion

This study investigates regional characteristics of CREs before and after the SCSSM onset using CERES-EBAF satellite and ERA-Interim data with a focus on the SCS and SC regions. The main conclusions are summarized as follows.

Before the SCSSM climatological onset pentad, weak precipitation and small amounts of cloud fractions occur over SCS, where low-level easterly wind and descending motion prevail; meanwhile, LWCRE, SWCRE, and NCRE are weak, but the TOA Rt is quite strong. In contrast, considerable amounts of precipitation and cloud

(C)1994-2021 China Academic Journal Electronic Publishing House. All rights reserved. http://www.cnki.net

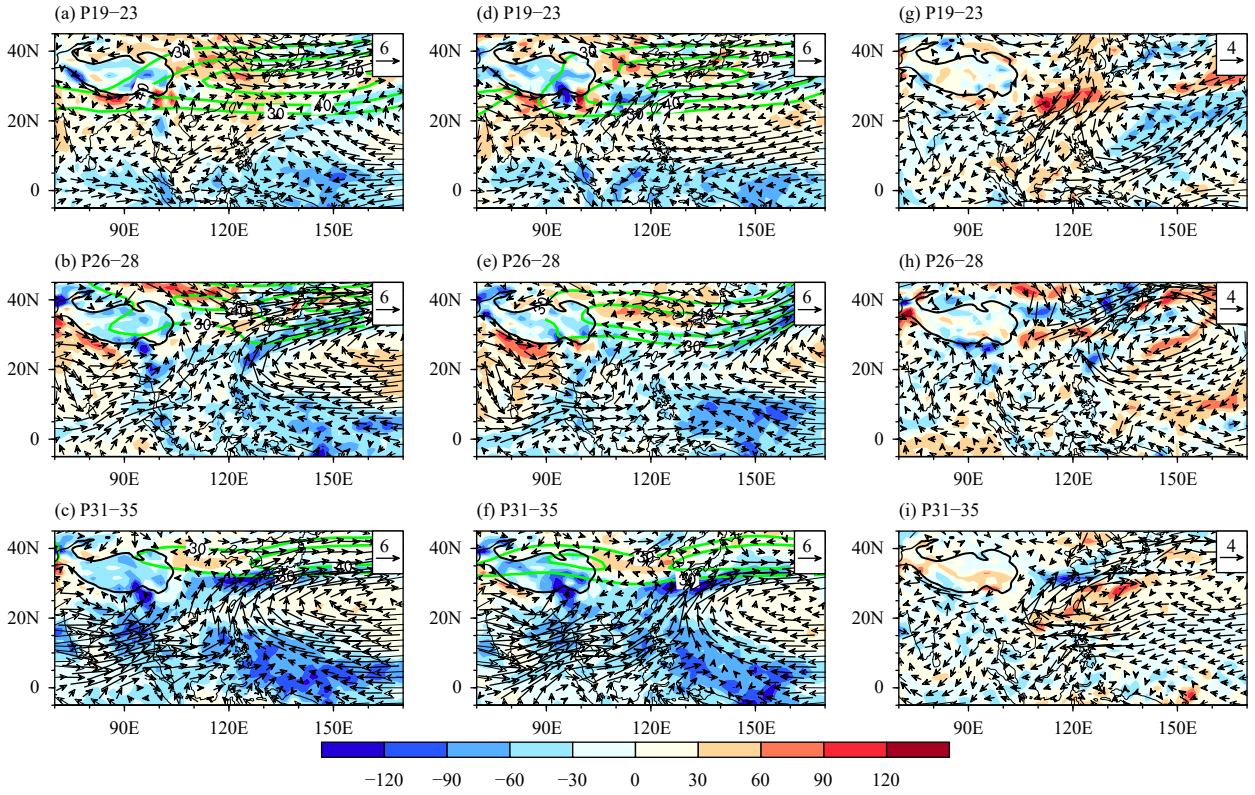

Fig. 10. Geographical distributions of circulation in (a) pentads 19−23, (b) pentads 26−28, and (c) pentads 31−35 in 2011; (d−f) the counterparts in 2012, and (g−h) their difference counterparts between 2011 and 2012. The shading is 500-hPa vertical velocity (hPa day^{-1}), the green line is 200-hPa westerly jet, and the vector is 850-hPa wind (m s^{-1}) masked below 850 hPa. The solid black line is the Tibetan Plateau (over 3000 m).

fractions accompanied by low-level southwesterly wind and moderate ascending motion occur over SC, where strong SWCRE (up to −120 W m^{-2}) dominates NCRE and the TOA Rt is much weaker than its counterpart over SCS.

In the SCSSM onset pentad, high and total clouds, LWCRE, and SWCRE abruptly increase over the southern and central SCS, accompanied by dramatical enhancement of low-level westerly wind, strong ascending motion, and sudden eastward movement of the western Pacific subtropical high. In the next pentads until mid-June, HCF, TCF, LWCRE, and SWCRE gradually increase over SCS, and their maximal centers display a northeastward movement mainly influenced by the western Pacific subtropical high. Because of the strong offset between LWCRE and SWCRE, the NCRE is still very weak over the SCS and Northwest Pacific regions, where TOA Rt therefore stays at a large-value level after the SCSSM onset. Over SC, HCF, LWCRE, and SWCRE gradually increase after the SCSSM onset although previous large amounts of low−middle-level clouds remain. In the meantime, cloud net radiative cooling (NCRE) gradually decreases, but TOA Rt shows an increasing trend over SC as a result of the more enhanced cloud radiative warming (LWCRE).

Case analyses further confirm the sharp contrast of cloud fractions, LWCRE, and SWCRE over SCS before and after the SCSSM onset. Moreover, the variations in the intensity and location of CREs are also sensitive to the distribution of large-scale circulation over the Asian summer monsoon regions. The results indicate that regional CREs are strongly modulated by quickly changed large-scale circulation over the Asian summer monsoon regions, and the variation of the former is a response to the variation of the later to a great degree. The ascending motion is a key connection between the local LWCRE and SWCRE intensity and the large-scale circulation over SCS. Another pronounced feature is that marked latitudinal differences in NCRE and Rt appear between SCS and SC, which mainly arise from their individual different cloud types and associated circulation conditions. These different characteristics of cloud fractions and CREs also exhibit discrepancies between the tropical SCSSM and the subtropical East Asian monsoon.

There are only 16-yr CERES-EBAF data, and in which only two consecutive case years are examined in this study. Many studies have pointed out that the circulation patterns associated with the SCSSM onset notice-

(C)1994-2021 China Academic Journal Electronic Publishing House. All rights reserved. http://www.cnki.net

ably differ in individual years (Wang et al., 2004; Kajikawa and Wang, 2012). Thus, the intensity and location of regional clouds and resultant CREs vary with the influencing circulation conditions. Moreover, cloud macro- and microphysics are influenced by many thermodynamic factors, and thus LWCRE (or SWCRE) does not fully match with the 500-hPa vertical motion shown in this study. Some studies have suggested that remarkable spring−summer differences in circulation conditions also occur between SCS and SC (He et al., 2007, 2008; Zhao et al., 2007, 2008). Therefore, it is necessary to further investigate the climatological and interannual characteristics of circulation and CREs over SCS, SC, and adjacent Asian monsoon regions before and after the SCSSM onset using more satellite and reanalysis data. In addition, this study focuses on examining observational features of regional CREs with the SCSSM onset, without investigating their possible feedbacks on evolution of the East Asian summer monsoon. In future work, well-designed model simulations will also be employed to explore the potential roles of CREs in the onset and advance of the SCSSM.

Acknowledgments. We thank Dr. Liang Wu for his constructive suggestions on the circulation analysis. CERES products used in this study are produced by the NASA CERES Team, available at http://ceres.larc.nasa.gov.

REFERENCES

Adler, R. F., G. J. Huffman, A. Chang, et al., 2003: The version-2 Global Precipitation Climatology Project (GPCP) monthly precipitation analysis (1979−present). *J. Hydrometeor.*, **4**, 1147–1167, doi: 10.1175/1525-7541(2003)004<1147:TVGPCP>2.0.CO;2.

Allan, R. P., 2011: Combining satellite data and models to estimate cloud radiative effect at the surface and in the atmosphere. *Meteor. Appl.*, **18**, 324–333, doi: 10.1002/met.285.

Bony, S., B. Stevens, D. M. W. Frierson, et al., 2015: Clouds, circulation and climate sensitivity. *Nat. Geosci.*, **8**, 261–268, doi: 10.1038/ngeo2398.

Boucher, O., D. Randall, P. Artaxo, et al., 2013: Clouds and aerosols. *Climate Change 2013: The Physical Science Basis. Contribution of Working Group I to the Fifth Assessment Report of the Intergovernmental Panel on Climate Change*. T. F. Stocker, D. Qin, G.-K. Plattner et al., Eds., Cambridge University Press, Cambridge, United Kingdom and New York, NY, USA, 571–657.

Cess, R. D., M. H. Zhang, B. A. Wielicki, et al., 2001: The influence of the 1998 El Niño upon cloud-radiative forcing over the Pacific warm pool. *J. Climate*, **14**, 2129–2137, doi: 10.1175/1520-0442(2001)014<2129:TIOTEN>2.0.CO;2.

Dee, D. P., S. M. Uppala, A. J. Simmons, et al., 2011: The ERA-Interim reanalysis: Configuration and performance of the data assimilation system. *Quart. J. Roy. Meteor. Soc.*, **137**, 553–597, doi: 10.1002/qj.828.

Ding, Y. H., and J. C. Chan, 2005: The East Asian summer monsoon: An overview. *Meteor. Atmos. Phys.*, **89**, 117–142, doi: 10.1007/s00703-005-0125-z.

Ding, Y. H., C. Y. Li, J. H. He, et al., 2006: South China Sea monsoon experiment (SCSMEX) and the East Asian monsoon. *J. Meteor. Res.*, **20**, 159–190.

Doelling, D. R., N. G. Loeb, D. F. Keyes, et al., 2013: Geostationary enhanced temporal interpolation for CERES flux products. *J. Atmos. Oceanic Technol.*, **30**, 1072–1090, doi: 10.1175/JTECH-D-12-00136.1.

Guo, Z., and T. T. Zhou, 2015: Seasonal variation and physical properties of the cloud system over southeastern China derived from CloudSat products. *Adv. Atmos. Sci.*, **32**, 659–670, doi: 10.1007/s00376-014-4070-y.

Hartmann, D. L., L. A. Moy, and Q. Fu, 2001: Tropical convection and the energy balance at the top of the atmosphere. *J. Climate*, **14**, 4495–4511, doi: 10.1175/1520-0442(2001)014<4495:TCATEB>2.0.CO;2.

He, J.-H., L. Qi, J. Wei, et al., 2007: Reinvestigations on the East Asian subtropical monsoon and tropical monsoon. *Chinese J. Atmos. Sci.*, **31**, 1257–1265, doi: 10.3878/j.issn.1006-9895.2007.06.20. (in Chinese)

He, J. H., P. Zhao, C. W. Zhu, et al., 2008: Discussions on the East Asian subtropical monsoon. *Acta Meteor. Sinica*, **66**, 683–696, doi: 10.3321/j.issn:0577-6619.2008.05.003. (in Chinese)

Hu, L., Y. D. Li, Y. Song, et al., 2011: Seasonal variability in tropical and subtropical convective and stratiform precipitation of the East Asian monsoon. *Sci. China Earth Sci.*, **54**, 1595–1603, doi: 10.1007/s11430-011-4225-y.

Huang, R., 1990: The East Asia/Pacific pattern teleconnection of summer circulation and climate anomaly in East Asia. *Climate Change Dynamics and Modeling*, China Meteorological Press, Beijing, 127–140.

Kajikawa, Y., and B. Wang, 2012: Interdecadal change of the South China Sea summer monsoon onset. *J. Climate*, **25**, 3207–3218, doi: 10.1175/JCLI-D-11-00207.1.

Kiehl, J. T., 1994: On the observed near cancellation between longwave and shortwave cloud forcing in tropical regions. *J. Climate*, **7**, 559–565, doi: 10.1175/1520-0442(1994)007<0559:OTONCB>2.0.CO;2.

Lau, K. M., and S. Yang, 1997: Climatology and interannual variability of the Southeast Asian summer monsoon. *Adv. Atmos. Sci.*, **14**, 141–162, doi: 10.1007/s00376-997-0016-y.

Lau, N.-C., and M. J. Nath, 2009: A model investigation of the role of air–sea interaction in the climatological evolution and ENSO-related variability of the summer monsoon over the South China Sea and western North Pacific. *J. Climate*, **22**, 4771–4792, doi: 10.1175/2009JCLI2758.1.

Li, J. D., W.-C. Wang, X. Q. Dong, et al., 2017: Cloud–radiation–precipitation associations over the Asian monsoon region: An observational analysis. *Climate Dyn.*, **49**, 3237–3255, doi: 10.1007/s00382-016-3509-5.

Li, J. D., W.-C. Wang, J. Y. Mao, et al., 2019: Persistent spring shortwave cloud radiative effect and the associated circulations over southeastern China. *J. Climate*, **32**, 3069–3087, doi: 10.1175/JCLI-D-18-0385.1.

Li, J. D., Q. L. You, and B. He, 2020: Distinctive spring short-

(C)1994-2021 China Academic Journal Electronic Publishing House. All rights reserved. http://www.cnki.net

wave cloud radiative effect and its inter-annual variation over southeastern China. *Atmos. Sci. Lett.*, **21**, e970, doi: 10.1002/asl.970.

Li, Z. N., S. Yang, B. He, et al., 2016: Intensified springtime deep convection over the South China Sea and the Philippine Sea dries southern China. *Sci. Rep.*, **6**, 30470, doi: 10.1038/srep30470.

Liu, X., A. Xie, and Q. Ye, 1998: The climatic characteristics of summer monsoon onset over South China Sea. *J. Trop. Meteor.*, **14**, 28–37. (in Chinese)

Loeb, N. G., B. A. Wielicki, D. R. Doelling, et al., 2009: Toward optimal closure of the Earth's top-of-atmosphere radiation budget. *J. Climate*, **22**, 748–766, doi: 10.1175/2008JCLI2637.1.

Luo, Y. L., R. H. Zhang, and H. Wang, 2009: Comparing occurrences and vertical structures of hydrometeors between eastern China and the Indian monsoon region using CloudSat/CALIPSO data. *J. Climate*, **22**, 1052–1064, doi: 10.1175/2008JCLI2606.1.

Pan, Z. X., W. Gong, F. Y. Mao, et al., 2015: Macrophysical and optical properties of clouds over East Asia measured by CALIPSO. *J. Geophys. Res. Atmos.*, **120**, 11653–11668, doi: 10.1002/2015JD023735.

Qian, W., and S. Yang, 2000: Onset of the regional monsoon over Southeast Asia. *Meteor. Atmos. Phys.*, **75**, 29–38.

Ramanathan, V., 1987: The role of earth radiation budget studies in climate and general circulation research. *J. Geophys. Res. Atmos.*, **92**, 4075–4095, doi: 10.1029/JD092iD04p04075.

Ren, S.-L. and X. Fang, 2013: The application of AMV and TBB in monitoring the South China Sea summer monsoon. *J. Trop. Meteor.*, **29**, 1051–1056. (in Chinese)

Rogers, R. R., and M. K. Yau, 1989: *A Short Course in Cloud Physics*. 3rd Ed., Butterworth-Heinemann, Woburn, 304 pp.

Tanaka, M., 1992: Intraseasonal oscillation and onset and retreat dates of the summer monsoon over East, Southeast Asia and the western Pacific region using GMS high cloud amount data. *J. Meteor. Soc. Japan*, **70**, 613–629.

Tao, S. Y., and L. X. Chen, 1987: A review of recent research on the East Asian summer monsoon in China. *Monsoon Meteorology*, C. P. Chang, and T. N. Krishinamurti, Eds., Oxford University Press, Oxford, 60–92.

Trenberth, K. E., J. T. Fasullo, and J. Kiehl, 2009: Earth's global energy budget. *Bull. Amer. Meteor. Soc.*, **90**, 311–324, doi: 10.1175/2008BAMS2634.1.

Wall, C. J., and D. L. Hartmann, 2018: Balanced cloud radiative effects across a range of dynamical conditions over the tropical West Pacific. *Geophys. Res. Lett.*, **45**, 11490–11498, doi: 10.1029/2018GL080046.

Wang, B., LinHo, Y. S. Zhang, et al., 2004: Definition of South China Sea monsoon onset and commencement of the East Asia summer monsoon. *J. Climate*, **17**, 699–710, doi: 10.1175/2932.1.

Webster, P. J., V. O. Magaña, T. N. Palmer, et al., 1998: Monsoons: Processes, predictability, and the prospects for prediction. *J. Geophys. Res. Oceans*, **103**, 14451–14510, doi: 10.1029/97JC02719.

Wu, G. X., Y. M. Liu, Q. Zhang, et al., 2007: The influence of mechanical and thermal forcing by the Tibetan Plateau on Asian climate. *J. Hydrometeor.*, **8**, 770–789, doi: 10.1175/JHM609.1.

Wu, R., and B. Wang, 2001: Multi-stage onset of the summer monsoon over the western North Pacific. *Climate Dyn.*, **17**, 277–289, doi: 10.1007/s003820000118.

Wu, R. G., 2002: Processes for the northeastward advance of the summer monsoon over the western North Pacific. *J. Meteor. Soc. Japan*, **80**, 67–83, doi: 10.2151/jmsj.80.67.

Yanai, M., S. Esbensen, and J. -H. Chu, 1973: Determination of bulk properties of tropical cloud clusters from large-scale heat and moisture budgets. *J. Atmos. Sci.*, **30**, 611–627.

Yu, R. C., Y. Q. Yu, and M. H., Zhang, 2001: Comparing cloud radiative properties between the eastern China and the Indian monsoon region. *Adv. Atmos. Sci.*, **18**, 1090–1102, doi: 10.1007/s00376-001-0025-1.

Zeng, Q. W., Y. Zhang, H. C. Lei, et al., 2019: Microphysical characteristics of precipitation during pre-monsoon, monsoon, and post-monsoon periods over the South China Sea. *Adv. Atmos. Sci.*, **36**, 1103–1120, doi: 10.1007/s00376-019-8225-8.

Zhang, B. C., Z. Guo, L. X. Zhang, et al., 2020: Cloud characteristics and radiation forcing in the global land monsoon region from multisource satellite data sets. *Earth Space Sci.*, **7**, e2019EA001027, doi: 10.1029/2019EA001027.

Zhao, P., R. H. Zhang, J. P. Liu, et al., 2007: Onset of southwesterly wind over eastern China and associated atmospheric circulation and rainfall. *Climate Dyn.*, **28**, 797–811, doi: 10.1007/s00382-006-0212-y.

Zhao, P., X. J. Zhou, L. X. Chen., et al., 2008: Characteristics of subtropical monsoon and rainfall over eastern China and western North Pacific and associated reasons. *Acta Meteor. Sinica*, **66**, 940–954, doi: 10.11676/qxxb2008.085. (in Chinese)

Zhu, C. W., X. J. Zhou, P. Zhao, et al., 2011: Onset of East Asian subtropical summer monsoon and rainy season in China. *Sci. China Earth Sci.*, **54**, 1845–1853, doi: 10.1007/s11430-011-4284-0.

Zhu, Q. G., J. R. Lin, S. W. Shou, et al., 2007: *Weather Principles and Methods*. 4th Ed., China Meteorological Press, Beijing, 649 pp. (in Chinese)

Tech & Copy Editor: Zhirong CHEN

(C)1994-2021 China Academic Journal Electronic Publishing House. All rights reserved. http://www.cnki.net